Forest Ecology and Management 269 (2012) 124–133

Contents lists available at SciVerse ScienceDirect

Forest Ecology and Management

journal homepage: www.elsevier.com/locate/foreco

Historic and future extent of wildfires in the Southern Rockies Ecoregion, USA

Sandra E. Litschert [a,*], Thomas C. Brown [b], David M. Theobald [c]

[a] Earth Systems Institute, 310 Mt Shasta Blvd. #6, Mount Shasta, CA 96067, United States
[b] Rocky Mountain Research Station, US Forest Service, Fort Collins, CO 80526, United States
[c] Dept. of Fish, Wildlife, and Conservation Biology, Warner College of Natural Resources, Colorado State University, Fort Collins, CO 80523-1474, United States

ARTICLE INFO

Article history:
Received 24 September 2010
Received in revised form 14 December 2011
Accepted 19 December 2011

Keywords:
Wildfires
Climate change
Downscaled climate data
Burned area model
Southern Rockies Ecoregion

ABSTRACT

Wildfires play a formative role in the processes that have created the ecosystems of the Southern Rockies Ecoregion (SRE). The extent of wildfires is influenced mainly by precipitation and temperature, which control biomass growth and fuel moisture. Forecasts of climate change in the SRE show an increase in temperatures, bringing warmer springs with earlier runoff and longer fire seasons. Increasing wildfire extent and intensity would affect human safety, livelihoods, and landscapes. Our summary of historical wildfire records from the national forests of the SRE from 1930 to 2006 revealed an order of magnitude increase in the annual number of fires recorded over the full time period and in the number of large fires since 1970. We developed a model of percent burned area in the SRE for the period 1970–2006 using temperature and precipitation variables ($R^2 = 0.51$, $p = 1.7E-05$). We applied this model to predict percent burned area using data from two downscaled global circulation models (GCMs), for the Intergovernmental Panel on Climate Change Special Report Emissions Scenarios A2 (projects high increases in temperature) and B1 (projects lower temperature increases), for the time period 2010–2070. The results showed increasing trends in median burned areas for all scenarios and GCM combinations with higher increases for the B1 scenario. The results suggest that precipitation increases could at least partially compensate for the effect of temperature increases on burned area but the strength of this ameliorating effect of precipitation will remain uncertain until the GCMs are further developed.

© 2011 Elsevier B.V. All rights reserved.

1. Introduction

Wildfires play a formative role in the Southern Rockies Ecoregion (SRE) by affecting plant and animal ecology, and geomorphic processes. Wildfires can also be disruptive socially by causing substantial losses of life and damage to property and resources (Graham, 2003). Property losses from wildfires are increasing as rural land is developed; indeed, 39% of houses in the conterminous US are now in the wildland–urban interface (Radeloff et al., 2005; Theobald and Romme, 2007). Wildfires can alter geomorphology and hydrology resulting in increased erosion and reduced water quality (EPA, 2000; Moody and Martin, 2001; Shakesby and Doerr, 2006), and costly maintenance of water storage and processing facilities (Palmieri et al., 2001; Graham, 2003). The increasing risk to property and other resources, and the growing need to use fire wisely to maintain ecological systems, both point to the importance of understanding how changes in the principal drivers of wildfire may alter the likelihood of future wildfires.

The occurrence and natural extent of SRE wildfires are mainly controlled by weather, in particular, temperature and precipitation, which affect structure, growth and moisture content of fuels (Gedalof et al., 2005; Cary et al., 2009). Topography also is important as elevation affects the amount and timing of precipitation; slope may increase the rate of fire spread as hot gases rise and preheat the upslope vegetation (Pyne et al., 1994). Climate change, by altering weather patterns, is likely to affect fire extent, frequency, and severity (Flannigan et al., 2005). Global scale studies suggest that climate change will alter spatial distributions of wildfires, causing increased likelihood of fires in some areas and decreases in other areas (Krawchuk et al., 2009).

In the western United States, patterns of fire occurrence are strongly related to seasonal changes in precipitation, temperature, and soil moisture for the fire year and one or more years prior to the fire, as these changes govern moisture availability for vegetative growth and for fuels (Bartlein et al., 2003; Littell et al., 2009). Warmer winter and spring temperatures during the 1980s and 1990s caused mountain snow to melt earlier and spring runoff to end sooner than in previous years (Westerling et al., 2006). For the time period 1977–2003 burned area was significantly and positively correlated with spring (defined as growing season) and summer temperatures (Littell et al., 2009). During this time period, fire seasons lengthened as fuels dried earlier (Westerling et al., 2006), the number of days of high fire danger in much of the West increased (Brown et al., 2004), and the numbers of wildfires and

* Corresponding author.
E-mail address: sam@earthsystems.net (S.E. Litschert).

0378-1127/$ - see front matter © 2011 Elsevier B.V. All rights reserved.
doi:10.1016/j.foreco.2011.12.024

area burned both increased due to changes in annual, seasonal, and monthly precipitation and temperature (Westerling et al., 2006; Balshi et al., 2009). Current year precipitation, especially summer and autumn precipitation, is also thought to control fuel moisture levels for the fire season (Drever et al., 2006; Westerling et al., 2006; Littell et al., 2009). Seasonal precipitation and temperature in the antecedent year can affect the growth of fine fuels and the moisture content of larger fuels (Brown et al., 2008; Littell et al., 2009).

Patterns of wildfire occurrence in the southwestern United States are related to longer-term climatic patterns of the El Nino Southern Oscillation (ENSO) (Swetnam and Betancourt, 1990), which is characterized by relatively moist El Niño years followed by drier La Niña years over periods of 2–7 years (Climate Prediction Center, 2005). Several years of above average precipitation can increase vegetative growth and similarly, several years of below-average precipitation can stress vegetation and dry large fuels (Swetnam and Betancourt, 1990; Westerling et al., 2003). These long-term effects may be particularly important in grassland and low elevation forests (Veblen et al., 2000). For example, in the ponderosa pine forests of the Colorado Front Range, herbaceous vegetation grows more prolifically during El Niño years with relatively high precipitation rates. This additional vegetative growth provides fine fuels that, when dried during the drier springs of La Niña years, encouraged the spread of wildfire (Veblen et al., 2000). Hence the inter-annual variability in moisture, generated by broad-scale ENSO cycles, can be more conducive to wildfires than drought alone (Veblen et al., 2000; Sibold et al., 2006).

In recent years, global circulation models (GCMs) characterizing the earth's climate have been refined to include regionally and temporally important factors such as ENSO (Cañon et al., 2007, 2011). Improvements in downscaling data from GCMs have generated data of fine enough spatial scale to be used as input to watershed-scale models (Hay et al., 2000; Wood et al., 2004; Cañon et al., 2011). Hence events such as wildfire, which are strongly influenced by weather, can be projected using the downscaled climate data.

The goals of this study were to summarize and analyze the historic wildfire extent in the SRE, to develop a model to predict the proportion of area burned, and to use the model to project the region's future extent of wildfire under climate change. We used downscaled climate data to improve the spatial resolution of previous studies that examined fires and climate change in the western United States (e.g. Westerling et al., 2006, and Spracklen et al., 2010); developed the model based on the relationship of climatic factors to area burned for the period 1970–2006; and used the model to estimate future burned area with downscaled climate forecasts from two global circulation models (GCMs) and two Intergovernmental Panel on Climate Change (IPCC) emissions scenarios: A2 (projects high increases in temperature) and B1 (projects lower temperature increases).

2. Description of the SRE

Our study area is defined as land within the SRE (Bailey et al., 1994) that is owned by the US Forest Service (41%, USFS) and Bureau of Land Management (12%, BLM). We included a 50 km buffer to prevent the edge effects commonly encountered in GIS processing and we call this area the SRE50. The SRE50 covers much of mountainous central Colorado plus parts of northern New Mexico and southern Wyoming in the United States, and comprises an area of almost 144,000 km^2 (Bailey et al., 1994) (Fig. 1). Elevations in the SRE50 range from 1000 to 4400 m. Mean annual precipitation for the years 1971–2000 ranges from 170 mm at the lower elevations to 1600 mm in the mountains. Mean annual temperatures

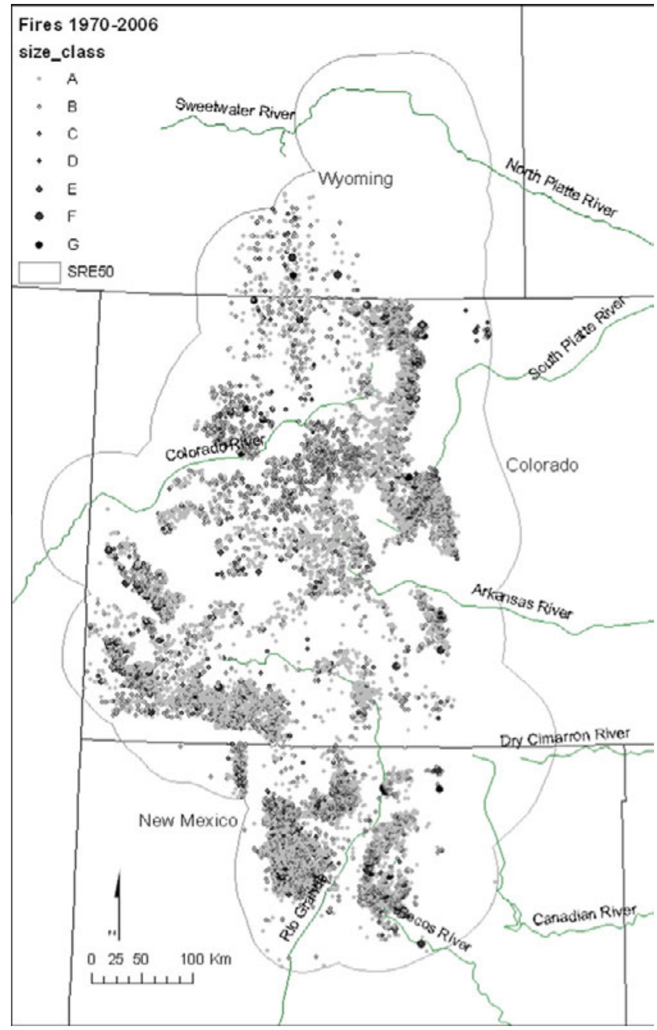

Fig. 1. Wildfire locations for the period 1970–2006 by fire size class in the Southern Rockies Ecoregion with a 50-km buffer (SRE50).

for 1970–2000 range from −4 to 13° C across the elevation range. Vegetation in the SRE includes prairie, shrublands, and pinyon-juniper woodlands at the lower elevations, mountain forests at the mid-elevations, and alpine tundra at the highest elevations. The SRE50 contains the headwaters of several major rivers of western and central North America, including the Colorado, Platte, Arkansas, and Rio Grande rivers.

3. Methods

Our goal in this study was to develop a model of the relationship of past weather to wildfire extent and use that model with projections of future weather to model possible future wildfire extent. All available spatial data for wildfires were obtained as point locations from eight national forests within the SRE50 for the period 1930–2006. The data obtained from the USFS also contained data from adjoining BLM lands. In addition, for large fires we obtained 95 fire polygons from the Geospatial Multi-agency Coordination (GEOMAC) website for 2000–2007.

The data required multiple processing steps before they could be used for model development. Fires in the GEOMAC dataset were deleted as suspected duplicates when a fire point within a fire polygon met at least two of the following three conditions: the same fire name, the same fire area or size class, and the same year of occurrence. We used centroids from the GEOMAC fire polygons to represent fire locations to match the fire points from the USFS data. The multiple GIS layers of fire incidence were appended to create a single burned area layer that contained the locations, fire size class or area burned, and year of the fire. About 4% of wildfires in this database were deleted because of missing attributes. The USFS designated seven fire size classes ranging from A (<0.001 km^2) to G (>20.2 km^2) (Table 1). For 2% of the fires only a size class was listed and these were assigned the median size for fires in that class.

Location precision remains a concern in decisions to include fires within the boundary of the SRE50 as methods for recording fire locations varied. About 34% of the points in the USFS data were hand-digitized from unknown data sources; 1% were originally located to the nearest quarter, half or full section by the Public Land Survey System; another 13% of the points were located using GPS or a combination of hand digitizing and GPS; and 17% were located using the Personal Computer Historical Analysis technique in the Fire Program Analysis System (USFS, 2006). The data sources of the remaining 35% of points are unknown. About 7% of the points were deleted because they appeared to be outside of federally owned lands that we used to calculate the total available land to burn. The potential lack of precision of the fire locations in the data may constrain modeling efforts that rely on those data.

Although data for our wildfire summary covers the full time period from 1930 to 2006 for which data are available, we restricted our modeling analysis to the 37-year period from 1970 to 2006. Data for years prior to 1970 were rejected because observation and detection of wildfires improved dramatically from 1930 to the 1960s, which skewed the burned area estimates towards later years. The remaining 1970–2006 period was judged to still be long enough to capture climate variability adequately. The resulting dataset contained 16,105 records of wildfires (Fig. 1). Note that we could not distinguish between human- and lightning-caused fires, as data on fire causes were not available for most of the fires. ArcGIS 9.3.1 (Esri™) was used for all spatial data analysis.

The response variable of our model was wildfire extent, which we characterized as the percentage of USFS and BLM land within the study area that burned in a given year (BA%). Because the BA% distribution is skewed, with large values being relatively uncommon, we log-transformed BA% to ensure a normal distribution when developing models relating weather to burned area.

Seasonal predictor variables were derived from monthly precipitation (mm) and temperature (°C) data available from PRISM (Daly et al., 1994) at a 4 km^2 resolution. Seasonal estimates were computed for the following 3-month periods, selected to match the temporal resolution of the GCM-based data: spring (April–June), summer (July–September), and autumn (October–December).

The 37-year historical record supports models with only a parsimonious set of predictor variables so that we limited our models to the six most important variables based on our literature review, factors that have been identified as important predictors of fire extent, and factors that embody the physical processes relevant to altered burned area. Short-term variables for the fire year and prior year affect fuel moisture and the growth of vegetation that becomes fine fuels. In contrast, the long-term averages may indicate the effect of long term drought on burned area. We selected spring temperature, and summer and autumn precipitation to represent weather in the fire year. To represent weather from the antecedent year, we selected previous autumn precipitation, as it had the most significant relationship with log-transformed percent area burned ($R^2 = 0.36$, $p = 0.0001$). To capture the effects of long-term weather patterns, we selected averages of the five prior year's precipitation and temperature as the usual oscillation period for ENSO is within 2–7 years with an average time period of 5 years (Climate Prediction Center).

We developed the global linear regression model with all six variables: the three current year variables, previous fall precipitation, and the two five prior year averages. Because only three of the six variables in the global model were significant at $p < 0.1$, we developed two more linear regression models that dropped variables in consecutive steps until all variables were significant. The first of these models, the short-term model, contains the four variables describing weather of the current and prior years: spring temperature, summer and autumn precipitation, and previous autumn precipitation. The other model, which we called the combined-term model, substitutes the two 5-year variables for two of the three current year variables, with the selection of the current year variable to include based on variable significance. The short-term model is intended to show the extent to which current and recent weather can explain burned area. The combined-term model tests the importance of bringing in longer-term weather data.

We tested for collinearity between variables using the variance inflation factor. Parameter coefficients were standardized to determine the importance of each variable to the model by subtracting the mean and dividing by the standard deviation. After standardizing it is possible to determine, using a one unit change in each variable, which variable causes the largest change in the response variable. Plots of residuals versus fitted values and normal QQ plots were used to determine if the models met assumptions of normality. We calculated Cook's distance to identify outliers. The Durbin–Watson statistic was calculated on model residuals to check for

Table 1
Distribution of the number of fires per fire area class for the SRE50 from 1930 to 2006 with median area, mean area, and area class limits (source of area classes: National Wildfire Coordinating Group). All fire areas are in km^2.

Fire area class	A	B	C	D	E	F	G			
Median fire area	0.0004	0.004	0.08	0.7	1.8	11	50			
Mean fire area	0.001	0.01	0.12	0.71	2.1	11	97			
Class fire area	<0.001	0.001–0.04	0.04–0.40	0.40–1.2	1.2–4.0	4.0–20.2	>20.2			
Time period	Numbers of fires per class							Total number of fires	Mean number of fires per year	Percent of total area burned per year
1930–1950	672	254	56	3	4	2	0	991	47	0.06
1951–1970	1283	797	53	9	5	0	0	2147	107	0.08
1971–1990	5374	2597	283	47	9	11	3	8324	416	0.75
1991–2006	4653	1721	183	44	34	13	19	6667	417	5.1
Totals	11,982	5369	575	103	52	26	22	18,129		
Percent of total number of fires	66	30	3.2	0.6	0.3	0.1	0.1			
Percent of total area burned	0.2	1.1	2.3	4.9	4.5	13	74			

Table 2
Fire data for the period 1970–2006 by land cover and land use area in the SRE50. Abbreviations used in the paper are shown in brackets.

LULC description	Percent of land area	Number of wildfires	Percent of burned area
Shrub/grassland steppe (ST)	43	1797	26
Low elevation forest (LEF)	12	4961	18
Mid elevation forest (MEF)	12	5794	26
High elevation forest (HEF)	6	1278	20
Lodgepole pine (LP)	2	872	7
Riparian/wetland (RW)	2	543	3
Other land covers/uses	22	853	N/A

temporal autocorrelation; a statistic of two indicates the absence of temporal autocorrelation as the statistic may range between 0 and 4 (S. Baggett, Rocky Mountain Research Station, US Forest Service, Pers. Comm., 2011). Ten-fold cross validation was used to determine the prediction error and hence the best model for use with future climate data. The R statistical package was used for all statistical analyses; we used the base, car, stats, and QuantPsyc packages (R Development Core Team, 2011. Version 2.13.1).

We initially intended to generate separate models by vegetation type because wildfire frequency and severity typically varies by vegetation type (Kilgore, 1981). We grouped land cover types in the LANDFIRE existing vegetation type (EVT) data (Landfire, 2006) into seven types (Table 2).[1] Over 95% of the fire location points for 1970–2006 occurred in the following six vegetation types, each with over 500 fires: lodgepole pine (*Pinus contorta*), low elevation forest, middle elevation forest, high elevation forest, riparian/wetland, and shrub/grassland steppe (Table 2). Consequently, our analysis was restricted to areas of public land within the SRE50 that contained fire data points and that were covered by one of these six vegetation types. The 900 m^2 EVT data were upscaled to 4 km^2 resolution to match the weather data using the majority class type. For each climate variable, averages were calculated over the area of the six vegetation types within the SRE50 for each year. We did not incorporate topographic variables because they would be unlikely to change in the relatively short time frame of the dataset.

Unfortunately, our attempts to develop sensible and significant models of burned area by vegetation type failed, most likely because of the coarse resolution of the wildfire data described above and the small area occupied by some of the vegetation types (Table 2). Consequently, we combined the data for the six vegetation types into a single model for the SRE50. Use of the single vegetation layer precluded the option of directly modeling fuels or accounting for recovery periods following fire.

The model with the lowest cross-validation prediction error was used to calculate future burned area using climate data from downscaled GCMs for years 2006–2070 to develop future estimates of the predictor variables. The UK Meteorological Office (UKMO) HadCM3 and the Max Planck Institute (MPI) ECHAM5 GCMs datasets were chosen from among 16 available GCM datasets because they best modeled the historic El Niño Southern Oscillation (ENSO) and Pacific Decadal Oscillation (PDO) weather patterns of the southwestern US (Dominguez et al., 2010). The downscaled GCM data were prepared by Cañon et al. (2011) at the 4 km^2 resolution using statistical methods.[2]

We selected downscaled weather data for the A2 and B1 emission scenarios which are designed to bracket the range in projected future temperature (Nakicenovic et al., 2000). The A2 scenario assumes that there will be high population growth with slow economic development and slow technological change, and generally results in relatively high increases in temperature (IPCC, 2007). The B1 scenario assumes that the global population peaks in the middle of the 21st century, and then declines, with economies becoming more service and information oriented (IPCC, 2007); this scenario generally results in relatively low temperature increases. With the two scenarios each modeled with the two GCMs, we have four scenario–GCM combinations.

Our comparison of PRISM and downscaled GCM data for years 2001–2010 indicated a bias in the GCM data. Hence the downscaled GCM data were adjusted by the difference (GCM minus PRISM) in the decadal averages for each variable. The bias correction resulted in, for example, differences of 149 mm and 179 mm being added to the ECHAM5 and HadCM3 A2 annual precipitation data, respectively, and differences of 1.9 and 2.5 °C being subtracted from the ECHAM5 and HadCM3 A2 annual temperature data, respectively. The historical and adjusted projected precipitation and temperature are shown in Fig. 2 for the A2 scenario.

Using the bias-corrected downscaled estimates of the selected weather variables, projections of BA% were computed for each GCM–scenario combination. The selected burned area model was used to estimate BA% for each year using the 60 years of projected weather variables for each of the four GCM–scenario combinations.

Given the right-skew of the BA% projections, the Kruskal–Wallis rank test was used to detect whether there were differences in BA% between the four future GCM–scenario combinations. As there were significant differences, the Wilcoxon rank-sum test was used to investigate these differences. Exponential trend lines were developed for each GCM–scenario as regressions with time. The overlaps were calculated for the standard error of slopes to determine significant differences between GCM–scenario combinations; an overlap between two combinations signifies no significant difference between combinations.

4. Results

We first summarize the historical fire record of the SRE50, showing changes in the number of fires and the fire size distribution over the 1930–2006 period. Then we present our models of burned area based on data for 1970–2006, showing how weather variables are related to burned area. Finally, we present the analysis of the effects of climate change on future burned area.

4.1. Wildfires 1930–2006

As seen in the fire size class distribution for the SRE50 area of Table 1, small fires are the most frequent, with classes A and B together accounting for 96% of all fires. The four largest classes (D, E, F, and G) together account for only 1% of the fires but 96% of the total fire area. The annual average number of recorded fires increased by an order of magnitude from the 1930s to the 2000s, from 47 wildfires per year for the period 1930–1950 to 417 for the period 1991–2006 (Table 1). The annual BA% also increased over the 1930–2006 period, rising from 0.06% in the earliest period to 5.1% in the most recent period (Table 1). The increase in burned

[1] The classification was performed using NatureServe Explorer, accessed in 2008 at: http://www.natureserve.org/explorer/.

[2] The downscaled data were obtained in 2008 at the following site: http://www.sahra.arizona.edu/research_data/SAHRAGeoDB.

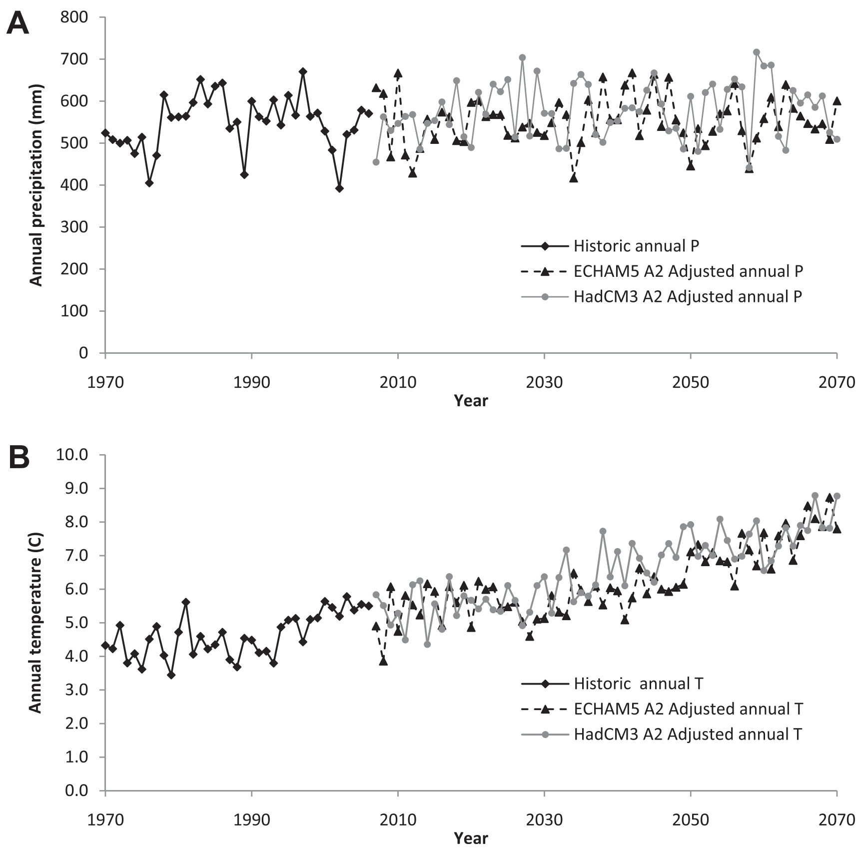

Fig. 2. Historic and projected annual precipitation and temperature. Historic data are from PRISM and projected data are from two GCMs and emission scenario A2.

area is evident in the distribution of fires by size class, as the number of large fires began increasing in the 1971–1990 period and increased further in the most recent time period (1991–2006). Since it is likely that large fires were always detected and reported, the data probably reflect a real increase in the number of large wildfires.

For all seven fire size classes, the mean fire area exceeds the median fire area, suggesting an overall skewed fire size distribution (Table 1). This is particularly true in unbounded class G where the mean fire area of 97 km^2 is nearly twice the median fire area (50 km^2).

During the 1970–2006 period, fires were most common in lower and drier forest areas, with 31% of the fires in low elevation forests and 36% in mid elevation forests, and least common in higher and/or wetter areas, with only 5% in lodgepole forests and 3% in riparian/wetland areas (Table 2). Burned area was greatest in shrub/steppe and mid elevation forest, which each contain 26% of the total burned area in the SRE50, and lowest in the lodgepole (7%) and riparian/wetland (3%) areas (Table 2).

4.2. The wildfire model

The global model, containing variables for spring temperature, summer precipitation, autumn precipitation, previous autumn precipitation, and the prior 5-year averages of both precipitation and temperature, was highly significant ($R^2 = 0.55$, $p = 0.00002$) (Table 3). The variance inflation factors for all variables in the global model were less than five indicating that collinearity did not exist between variables (S. Baggett, Rocky Mountain Research Station, US Forest Service, pers. Comm., 2011). Three variables in the global model, spring temperature, 5-year precipitation and 5-year temperature, were not significant at $p < 0.05$ and became candidates for removal from the model to reduce redundancy.

Dropping the two 5-year variables from the global model produces the short-term model, which is highly significant ($R^2 = 0.52$, $p = 0.00001$) with all variables significant at $p < 0.1$. Dropping the two non-significant variables of the global model, spring T and autumn P, produces the combined-term model ($R^2 = 0.51$; $p = 0.00002$) (Table 3). In both models, as would be expected, greater burned area is associated with lower summer and previous autumn precipitation. In addition, in the combined-term model, greater burned area is associated with higher prior 5-year temperature and precipitation. A higher long-term prior temperature would tend to dry both large downed fuels and live vegetation. A higher long-term prior precipitation would tend to enhance the growth of small vegetation that could then assist fire ignition and spread.

Diagnostic plots showed normally distributed residuals and normal Q–Q plots meaning that all models meet assumptions of normalcy (see Fig. 3a for plots of the combined-term model). Similarly, the historic values were within the 95% prediction intervals of the models for all but a few extreme years (Fig. 3b). The Cook's distance calculated for each model prediction showed that no data point was overly influential, i.e., $D < 1$ for all data in all models. We found no temporal autocorrelation in residuals of the models using the Durbin–Watson statistic which ranged from 2.3 to 2.5 across the three models.

Although all three models are highly significant, with positive or negative signs on the coefficients of the independent variables that concur with our interpretations of the physical effects of the variables on fire area, the short-term and combined-term models have the advantage of parsimony over the global model. The cross validation (CV) error suggests a slight preference for the

Table 3
Summaries of predictor variables for (a) short-term model, (b) combined-term model, (c) global model, and (d) model statistics. P = precipitation (mm), T = temperature (°C).

	Estimate	Standard error	Standardized coefficients	t value	Pr(>|t|)
(a) Short term					
Intercept	−2.365	0.904		−2.616	0.013
Spring T	0.221	0.085	0.36	2.591	0.014
Summer P	−0.007	0.002	−0.34	−2.883	0.007
Previous autumn P	−0.007	0.002	−0.40	−2.946	0.006
Autumn P	−0.004	0.002	−0.23	−1.892	0.068
(b) Combined term					
Intercept	−4.166	1.348		−3.089	0.004
Summer P	−0.008	0.002	−0.41	−3.280	0.003
Previous autumn P	−0.010	0.002	−0.61	−5.153	0.000
P5 yr	0.003	0.002	0.22	1.795	0.082
T5 yr	0.421	0.176	0.29	2.390	0.023
(c) Global					
Intercept	−4.401	1.336		−3.295	0.003
Spring T	0.142	0.093	0.23	1.534	0.136
Summer P	−0.008	0.002	−0.41	−3.486	0.002
Autumn P	−0.004	0.002	−0.22	−1.924	0.064
Previous autumn P	−0.008	0.002	−0.48	−3.494	0.002
P5 yr	0.003	0.002	0.19	1.619	0.116
T5 yr	0.318	0.191	0.22	1.666	0.106

(d)	Standard error	Degrees of freedom	R^2	Adjusted R^2	F	P value	Durbin–Watson	Cross validation error
Short term	0.46	32	0.57	0.52	11	1.3E-05	2.3	0.241
Combined term	0.47	32	0.56	0.51	10	1.7E-05	2.4	0.238
Global	0.45	30	0.63	0.55	8.4	2.3E-05	2.5	0.239

combined-term model (CV error = 0.238) over the short-term model (CV error = 0.241). A further advantage of the combined-term model over the short-term model is that longer-term processes are also captured in the combined-term model. In that model, variables for the fire year and previous year account for seasonal fuel moisture and the abundance of fine fuels through vegetation growth, particularly in grassland and low elevation forests where the fire frequency is high and long term variables account for the effects of long-term drought as temperature and precipitation combine to affect the moisture content of larger downed fuels and trees.

4.3. Climate change and wildfires

4.3.1. Comparison of historical and modeled burned area

For the B1 scenario, the median annual BA% projections, which are 0.63% with the ECHAM5 climate model and 0.52% with the HadCM3 model, are several times the historic rate of 0.11% (Table 4). The increase in BA% for the B1 scenario probably occurs because the drier summers and previous autumns would result in drier fine fuels (Westerling et al., 2006). Similarly, the five prior year temperatures increased by 1.6 °C above those of the historic climate and this would cause large fuels to be drier than in cooler temperatures (Table 4). Despite the increase in median values, the maximum BA%s for both GCMs are actually less than the historic high of 7.5%, indicating either that the B1 climate does not include the extreme values that could replicate the historic maximum or that the model does not account for the pattern of climate values that cause extreme BA% values.

Results for the A2 scenario showed slightly smaller increases in median BA% than for the B1 scenario, with median BA%s of 0.50% with the ECHAM5 climate model and 0.32% with the HadCM3 model (Table 4). The maximum values are more complex as the ECHAM5 maximum is only 6.2% which is lower than the historic maximum, but the HadCM3 maximum value is 9.2%, an increase of 22% over the historic maximum. The HadCM3 A2 maximum may result from higher overall values for precipitation which could increase the growth of fine vegetation in previous years, leading to more fuels and higher average temperatures resulting in drier fuels.

4.3.2. Comparison of modeled burned area between GCMs and between climate scenarios

Differences in projected BA% among the four GCM–scenario combinations were found to be significant using the Kruskal–Wallis rank-sum test (chi-square = 13.07, p = 0.004). Between models for the A2 scenario, the ECHAM5 projections were significantly higher than the HadCM3 projections (W = 1261, p = 0.01) using the Wilcoxon test. The lower HadCM3–A2 projections may be attributed to the generally wetter weather, with increases of up to 16% for the precipitation variables above ECHAM5–A2 precipitation (Table 4). The two B1 scenario results were not significantly different from each other (p = 0.3).

Projections of annual BA% were significantly lower for HadCM3–A2 than for HadCM3-B1 (W = 2179, p = 0.02). Although the HadCM3–A2 combination had the highest maximum values, the projections of BA% were mainly lower than those of the other GCM–scenario combinations (Fig. 3c). Although the HadCM3–A2 combination had the highest prior 5-year average temperature, it was on average wetter than the other combinations (Table 4). Projected BA% of the two scenarios using the ECHAM5 model were not significantly different (p = 0.4).

Trend line slopes show significant increases for all GCM–scenario combinations (p < 0.01) and the overlapping standard error intervals on trend line slopes indicate that there is no significant difference between the increases in BA% for the HadCM3–A2 scenario, and both ECHAM5 scenarios (Fig. 3c).

5. Discussion

Changes in the history of wildfire in the SRE are indicative of human presence in the US West, changing patterns of management including fire detection and fire suppression, and climate. However, in recent years, the extent of burned areas in the SRE50 has been unusually high, with increases in burned area extent several times that of previous decades, suggesting that climate change is affecting wildfire extent, indicating the need to examine the fire record, and to model wildfire. Burned area projections suggest that further increases are likely and this finding is particularly

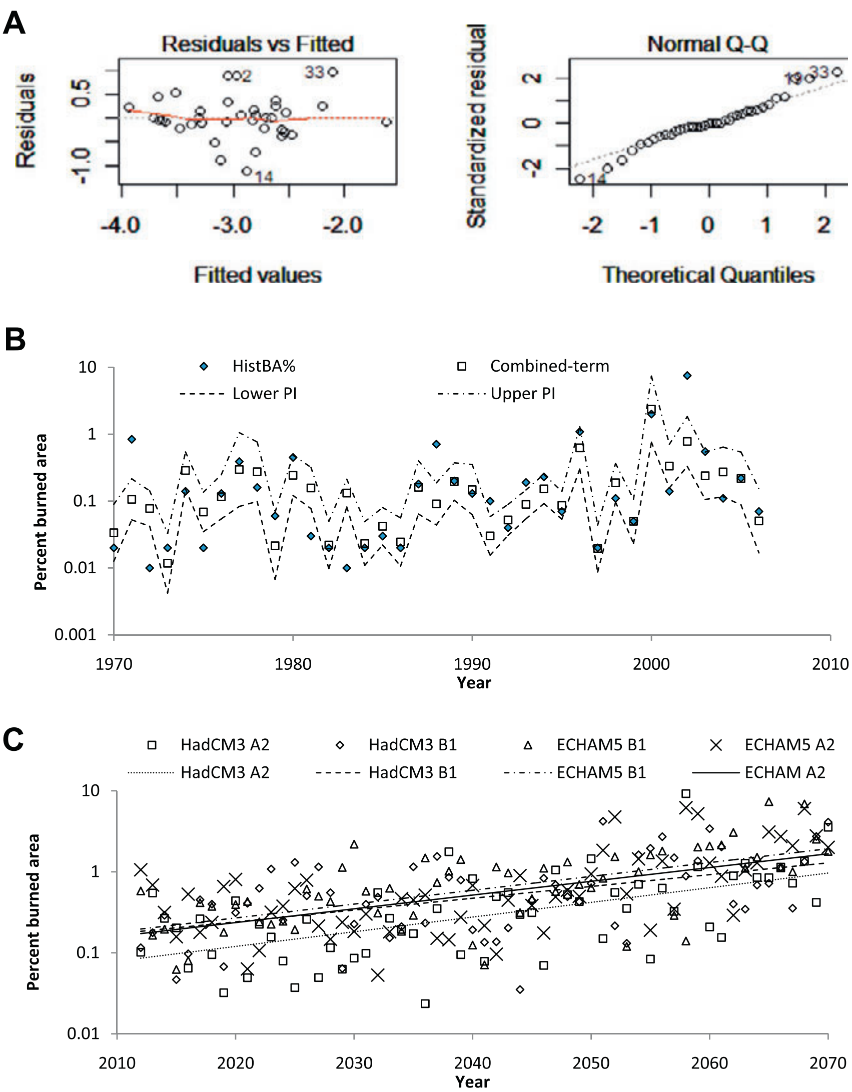

Fig. 3. (a) Diagnostic plots for the combined-term model, (b) historic percent burned area (BA%), model predictions, and 95% prediction intervals for the combined-term model and (c) projected burned area (BA%) for the combined-term model showing percent burned area for the SRE for GCMs:HADCM3 and ECHAM5 and IPCC scenarios: A2 and B1.

Table 4
Historic percent burned area (1970–2006) compared to projected annual burned area using the combined-term model with data from four GCM–climate scenario combinations (2010–2070) with climate averages for predictor variables. P = precipitation (mm), T = temperature (°C).

Burned area	Historic	HadCM3 B1	HadCM3 A2	ECHAM5 B1	ECHAM5 A2
Median	0.11	0.52	0.32	0.63	0.50
Minimum	0.01	0.04	0.02	0.06	0.05
Maximum	7.54	6.15	9.21	7.33	6.16
Mean	0.44	1.03	0.65	1.06	1.03
Standard deviation	1.26	1.28	1.21	1.34	1.41
Climate averages					
Summer P	156	178	190	149	166
Previous autumn P	132	115	148	128	127
5 yr average P	545	544	578	524	552
5 yr average T	4.6	6.2	6.4	6.3	6.2

important because of the increasing numbers of people and structures moving into the wildland–urban interface. Land managers will need to understand how to allocate resources and manage fuels for protection.

Studies of the effects of historic and future climate on wildfire have successfully used a variety of explanatory variables such as monthly precipitation and temperature (e.g., Flannigan et al., 2005; Drever et al., 2009), seasonal precipitation and temperature (e.g., Westerling et al., 2006; Brown et al., 2008; Littell et al., 2006), fire weather indices (e.g., Trouet et al., 2008; Spracklen et al., 2010), dry spells (Drever et al., 2006), fuel moisture (Flannigan et al., 2005), and metrics of the El Nino Southern Oscillation and the

Pacific Decadal Oscillation (e.g., Brown et al., 2008). In a study that used HadCM3 data that had not been downscaled, Drever et al. (2006) found that monthly temperature maxima during the fire season and dry spell sequences in Quebec explained variation in area burned and that increased temperatures using HadCM3–A2 data led to a significant increase in burned area. In contrast the results of this study suggest that the HadCM3–A2 combination produced the lowest burned area values (Fig. 3c and Table 4). The differences may be explained by the spatial variation in climate and wildfire regime between Quebec and the SRE.

Wildfire area in the western United States was 6.5 times greater from the mid-1980s to 2003 than from 1970 to 1986 (Westerling et al., 2006), which is very similar to our finding for the SRE50 of a 5.5-fold increase in percent burned area over the same time period, suggesting similarities between the SRE and average western conditions. For the Northern and Southern Rocky Mountains, Spracklen et al. (2010) report a much lower annual average burned area percentage of 0.02% for the period 1996–2005 than we found for the SRE50 (1.18%). This difference between our findings and Spracklen et al.'s may partially result from the fact that Spracklen et al. (and Westerling et al.) included only fires greater than 400 ha whereas we also included smaller fires. Perhaps more important, Spracklen et al.'s study includes large areas of subalpine fir in the Northern Rockies, which is comparable to high elevation forest and lodgepole pine in the southern Rockies and these forest types account for only about one quarter of the SRE50 area. The dominant vegetation types in the SRE50 are the shrub/steppe, low elevation forest, and mid-elevation forest, which together comprise 70% of the area (Table 2). Subalpine fir and high elevation forest/lodgepole pine burn much less frequently than do the dominant SRE50 vegetation types, resulting in a lower mean burned area for the Rockies as a whole than for the SRE50. Spracklen et al. (2010) projected that average annual burned area in the Rockies for 2046–2055 would double in comparison to the 1996–2005 decade, while our projections for the same time period for the SRE50 remain very similar to the 1996–2005 average; this discrepancy may occur because the SRE50 historical data contained three of the largest wildfire area records on history for the SRE50.

Interestingly, a recent change in fire management has implications for the interpretation of our results. Beginning in the early decades of the 20th century, wildfires were actively suppressed by public land management agencies. These years of fire exclusion and suppression probably altered the structure, composition and fuel loadings of forests, which may have increased the potential for wildfire (Kauffman, 2004; Stephens, 2005) especially in low elevation forests, which have a shorter fire return interval than subalpine and lodgepole pine forests (Romme et al., 2006). However, the perceptions of the role of fire and fire management have changed radically, resulting in greater recognition of a beneficial role of wildfire in maintaining heterogeneity in many forest and grassland ecosystems (Bisson et al., 2006). The changes in wildfire management have been relatively recent and may not yet have had an appreciable effect on fire incidence in the SRE50. Our projections of future burned area under climate change will overestimate burned area to the extent that the changes in policy are effective in altering future fire patterns compared with the 1970–2006 period.

The accuracy of the burned area model developed here is limited by the 1970–2006 fire data in three ways. First, we did not distinguish between human- and lightning-caused fires, as fire cause was not listed for most fires in the data set. Human-caused fires tend to occur along highways and near developed areas, so they may not reflect weather patterns as clearly as do lightening caused fires (Bartlein et al., 2003, 2008). Second, the coarse resolution of the fire data may limit the accuracy of the burned area model because fire points were located by different methods with varying levels of accuracy and precision. Thirdly, since we needed to know fire area, for the 4% of the fire points without a listed fire area, we assigned a fire area equal to the median of the fires in the respective fire size class.

The burned area model is based on a summary of wildfire data at the ecoregion level which is coarse but this was necessitated by the inability to model at the scale of individual vegetation types as mentioned earlier. Modeling at such a coarse scale overlooks the fine scale spatial patterns in vegetation types, precipitation, and fire incidence that are important for forest management at the watershed scale. However, the goal of this research was to provide a regional analysis with a long-term perspective that might anticipate the effects that future climates might have on area of wildfires in the Southern Rockies Ecoregion. We do not intend our results to be applied to watershed-level management questions. Hence, in constructing the model at the ecoregional scale, we have assumed that all vegetation types have an equal probability of burning and this means that the results apply mostly to shrub, grassland, and low to mid elevation forests as these comprise the largest land cover area in the Southern Rockies Ecoregion.

A potential concern with the burned area model because it was developed from time series data, is the effect of previously burned areas on burned area in the current year. This was not expected to be a serious concern for two reasons. First, very little of the total area burned in a given year, such that nearly all of the area had not experienced a recent fire. Second, it is physically possible that areas prone to frequent fires, such as grasslands and low elevation forests, could burn repeatedly over a small number of years. For example, areas within the Hayman fire had burned two or three times during the prior 12 years (Graham, 2003).

Uncertainty of model-based estimates increases with the use of input data that are themselves modeled. Although the climate data sets provide the best available data for our purposes, both data sources provide modeled estimates that necessarily rely on assumptions. Uncertainty in the PRISM data comes from the interpolation of measured precipitation data and regression equations based on local topography (Daly et al., 1994). GCMs model regional climate at large scale; the estimates are then downscaled statistically to account for local spatial and temporal variations. Use of the statistically downscaled GCM data is limited by the mathematics of central tendencies and it is not clear how well these datasets capture the extremes of future weather.

Uncertainties remain regarding the relative contributions of past fire suppression and the beginnings of climate change to past burned area trends in the SRE50. Accurately separating the effects of vegetation and climate change would require more detailed data than were available, with fuel management or treatment histories to match the timeline of wildfires and weather related variables. Precipitation is highly varied and difficult to predict in this semi-arid, high relief region; GCMs do not yet consistently predict precipitation trends in Colorado (Ray et al., 2008). However all GCMs agree that temperature and potential evapotranspiration will increase, leading to decreased runoff and soil moisture (Ray et al., 2008) and suggesting increases in burned area. As climate change progresses, researchers will be able to obtain more data on the likely trends and magnitudes of precipitation and temperature and further refine burned area models.

The burned area model developed here is specific to the SRE50 but the methodology could be applied in other areas to understand the broad effects of future climate on burned area. Further, the burned area model could be improved by incorporating a fire-spread model to determine specific burned areas, and by accounting for fire recovery periods, allowing vegetation to recover and progress through seral stages. This improvement would provide a more realistic approach to understanding the likely effect of climate change on vegetation and determining the ability of forests to re-grow.

6. Conclusion

The period from 1930 to 2006 saw an increase of two orders of magnitude in the numbers and burned areas of wildfires in the SRE50, with some exceptionally large fires in recent years. Although some of this increase can be attributed to improved fire detection, most is probably due to an increase in the incidence of human-caused fires and to unusually hot and dry weather during the latter years of the period. Based on the projections of our burned area model, that represents the effects of precipitation and temperature on BA% in the SRE50, the median annual burned area over the period 2010–2070 may increase by between two and five times depending on which GCM–climate scenario combination most accurately characterizes future conditions. Given that human population in the WUI is very likely to increase in the future (Theobald and Romme, 2007), the pressures for enhanced management of fires and fuels will probably intensify regardless of how the climate changes. These pressures will be further amplified if, as indicated by our results, burned area also increases as the climate changes in comparison with the recent past. If future precipitation is greater than in the recent past, as indicated by the climate model simulations for the A2 scenario, those precipitation increases can lessen, though not necessarily balance, the effects of temperature increases, thereby ameliorating the weather-based amplification of pressures on forest and wildfire managers. We must await improvements in climate modeling before we can remove this uncertainty about future precipitation and thus about future burned area.

Acknowledgments

This research was supported in part by funds from the Rocky Mountain Research Station, US Forest Service. The authors thank in particular Scott Baggett of the RMRS for his patient help with statistics and the use of the R statistic package. Also we thank John B. Norman, Jessica Salo, and Carol Miller for their help, and Robert Keane and two other anonymous reviewers for their thoughtful suggestions.

References

Bailey, R.G., Avers, P.E., King, T., McNab, W.H., 1994. In: McNab, W.H., Bailey, R.G. (Eds.), Ecoregions and Subregions of the United States (Map): 1:1:7,500,000 (with Supplementary Table of Map Unit Descriptions). US Forest Service, Washington, DC.

Balshi, M.S., Mcguire, A.D., Duffy, P., Flannigan, M., Walsh, J., Melillo, J., 2009. Assessing the response of area burned to changing climate in western boreal North America using a Multivariate Adaptive Regression Splines (MARS) approach. Global Change Biol. 15, 578–600. doi:10.1111/j.1365-2486.2008.01679.x.

Bartlein, P.J., Hostetler, S.W., Shafer, S.L., Holman, J.O., Solomon, A.M., 2003. The seasonal cycle of wildfire and climate in the western United States. In: Fifth Symposium on Fire and Meteorology. American Meteorological Society, Orlando, FL, pp. 3.9-1–3.9-6.

Bartlein, P.J., Hostetler, S.W., Shafer, S.L., Holman, J.O., Solomon, A.M., 2008. Temporal and spatial structure in a daily wildfire-start data set from the western United States (1986–96). Int. J. Wildland Fire 17, 8–17.

Bisson, P.A., Buffington, J.M., Montgomery, D.R., 2006. Valley segments, stream reaches, and channel units. In: Hauer, F.R., Lamberti, G.A. (Eds.), Methods in Stream Ecology. Academic Press, Burlington, MA, p. 877.

Brown, T.J., Hall, B.L., Westerling, A.L., 2004. The impact of twenty-first century climate change on wildland fire danger in the western United States: an applications perspective. Clim. Change 62, 365–388.

Brown, P.M., Heyerdahl, E.K., Kitchen, S.G., Weber, M.H., 2008. Climate effects on historical fires (1630-1900) in Utah. Int. J. Wildland Fire 17, 28–39.

Cañon, J., González, J., Valdéz, J., 2007. Precipitation in the Colorado River Basin and its low frequency associations with PDO and ENSO signals. J. Hydrol. 333, 252–264.

Cañon, J., Dominguez, F., Valdéz, J.B., 2011. Downscaling climate variability associated with quasi-periodic climate signals: a new statistical approach using MSSA. J. Hydrol. 398 (1–2), 65–75.

Cary, G.J., Flannigan, M.D., Keane, R.E., Bradstock, R.A., Davies, I.D., Lenihan, J.M., et al., 2009. Relative importance of fuel management, ignition management and weather for area burned: evidence from five landscape-fire-succession models. Int. J. Wildland Fire 18, 147–156.

Climate Prediction Center, 2005. Available from: <http://www.cpc.ncep.noaa.gov/products/analysis_monitoring/ensostuff/ensofaq.shtml> (accessed November 2010).

Daly, C., Neilson, R.P., Phillips, D.L., 1994. A statistical-topographic model for mapping climatological precipitation over mountainous terrain. J. Appl. Meterol. 33, 140–160.

Dominguez, F., Cañon, J., Valdéz, J., 2010. IPCC-AR4 climate simulations for the Southwestern US: the importance of future ENSO projections. Clim. Change 99, 499–514.

Drever, C.R., Bergeron, Y., Drever, M.C., Flannigan, M., Logan, T., Messier, C., 2006. Effects of climate change on occurrence and size of large fire in a northern hardwood landscape: historical trends, forecasts, and implications for climate change in Temiscamingue, Quebec. Appl. Veget. Sci. 12, 261–272.

EPA, 2000. National Water Quality Inventory, 1998 Report to Congress. Environmental Protection Agency, Washington, DC.

Flannigan, M., Logan, K., Amiro, B., Skinner, W., Stocks, B., 2005. Future area burned in Canada. Clim. Change 72, 1–16.

Gedalof, Z., Peterson, D., Mantua, N., 2005. Atmospheric, climatic, and ecological controls on extreme wildfire years in the northwestern United States. Ecol. Appl. 15 (545), 154–174.

Graham, R.T. (Ed.), 2003. Hayman Fire Case Study. General Technical Report RMRS-GTR-114. Rocky Mountain Research Station, US Forest Service, Ogden, UT.

Hay, L.E., Wilby, R.L., Leavesley, G.H., 2000. A comparison of delta change and downscaled GCM scenarios for three mountainous basins in the United States. J. Am. Water Res. Assoc. 36 (2), 387–397.

IPCC, 2007. Climate Change 2007: Synthesis Report. IPCC, Geneva, Switzerland. Available from: <http://www.ipcc.ch/ipccreports/ar4-syr.htm>.

Kauffman, J.B., 2004. Death rides the forest: perceptions of fire, land use, and ecological restoration of Western forests. Conserv. Biol. 18, 878–882.

Kilgore, B., 1981. Fire in ecosystem distribution and structure: western forests and scrublands. In: Mooney, H.A., Bonnicksen, T.M., Christensen, N.L. (Eds.), Proceedings of the Conference: Fire Regimes and Ecosystem Properties. General Technical Report WO-GTR-26, US Forest Service, pp. 58–89.

Krawchuk, M.A., Moritz, M.A., Parisien, M.A., Dorn, J.V., Hayhoe, K., 2009. Global pyrogeography: the current and future distribution of wildfire. PLoS ONE 4, E5102, doi:5110.1371/journal.pone.0005102.

Landfire, 2006. The National Map LANDFIRE: LANDFIRE National Existing Vegetation Type Layer. US Department of Interior, Geological Survey.

Littell, J.S., McKenzie, D., Peterson, D.L., Westerling, A.J., 2009. Climate and wildfire are burned in western US ecoprovinces, 1916–2003. Ecol. Appl. 19 (4), 1003–1021.

Moody, J.A., Martin, D.A., 2001. Initial hydrologic and geomorphic response following a wildfire in the Colorado Front Range. Earth Surf. Process. Landforms 26, 1049–1070.

Nakicenovic, N., Alcamo, J., Davis, G., Vries, B.D., Fenhann, J., Gaffin, S., 2000. Emissions Scenarios: A Special Report of Working Group III of the Intergovernmental Panel on Climate Change. Cambridge University Press, Cambridge, UK, http://www.grida.no/climate/ipcc/emission/index.htm.

Palmieri, A., Shah, F., Dinar, A., 2001. Economics of reservoir sedimentation and sustainable management of dams. J. Environ. Manage. 61, 149–163.

Pyne, S.J., Andrews, P.L., Laven, R.D., 1994. Introduction to Wildland Fire. Wiley and Sons, New York, 455pp.

R Development Core Team, 2011. R: A Language and Environment for Statistical Computing. R Foundation for Statistical Computing, Vienna, Austria.

Radeloff, V.C., Hammer, R.B., Stewart, S.I., Fried, J.S., Holcom, S.S., Mckeefry, J.F., 2005. The wildland–urban interface in the United States. Ecol. Appl. 15, 799–805.

Ray, A.J., Barsugli, J.J., Averyt, K.B., 2008. Climate Change in Colorado: A Synthesis to Support Water Resources Management and Adaptation. Western Water Assessment, University of Colorado, Boulder, p. 58.

Romme, W.H., Clement, J., Hicke, J., Kulakowski, D., MacDonald, L.H., Schoennagel, T.L., et al., 2006. Recent Forest Insect Outbreaks and Fire Risk in Colorado Forests: A Brief Synthesis of Relevant Research. Colorado Forest Restoration Institute, Colorado State University, Fort Collins, CO.

Shakesby, R.A., Doerr, S.H., 2006. Wildfire as a hydrological and geomorphological agent. Earth Sci. Rev. 74, 269–307.

Sibold, J.S., Veblen, T.T., Gonzalez, M.E., 2006. Spatial and temporal variation in historic fire regimes in subalpine forests across the Colorado Front Range in Rocky Mountain National Park, Colorado, USA. J. Biogeogr. 32, 631–647.

Spracklen, D.V., Mickley, L.J., Logan, J.A., Hudman, R.C., Yevich, R., Flannigan, M.D., Westerling, A.J., 2010. Impacts of climate change from 2000 to 2050 on wildfire activity and carbonaceous aerosol concentrations in the western United States. J. Geophys. Res. 114, D20301. doi:10.1029/2008JD010966.

Stephens, S.L., 2005. Forest fire causes and extent on United States Forest Service lands. Int. J. Wildland Fire 14, 213–222.

Swetnam, T.W., Betancourt, J.L., 1990. Fire-southern oscillations relations in the southwestern United States. Science 249, 1017–1020.

Theobald, D.M., Romme, W.H., 2007. Expansion of the US wildland–urban interface. Landscape Urban Plann. 83, 340–354.

Trouet, V., Taylor, A.H., Carleton, A., Skinner, C.N., 2008. Interannual variations in fire weather, fire extent, and synoptic scale circulation patterns in northern California and Oregon. Theor. Appl. Climatol. 95, 349–360.
USFS, 2006. Personal Computer Historic Analysis (PCHA) Users' Guide. Available from: <http://www.fs.fed.us/fire/planning/nist/PCHA_Users_Guide_3_23_2006.pdf> (accessed 2010).
Veblen, T.T., Kitzberger, T., Donnegan, J., 2000. Climatic and human influences on fire regimes in ponderosa pine forests in the Colorado Front Range. Ecol. Appl. 10, 1178–1195.
Westerling, A.L., Brown, T.J., Gershunov, A., Cayan, D.R., Dettinger, M.D., 2003. Climate and Wildfire in the western United States. Bull. Amer. Meteor. Soc. 84 (5), 595–604.
Westerling, A.L., Hidalgo, H.G., Cayan, D.R., Swetnam, T.W., 2006. Warming and earlier spring increases western US forest wildfire activity. Science 313, 940–943.
Wood, A.W., Leung, L.R., Sridhar, V., Lettenmaier, D.P., 2004. Hydrologic implications of dynamical and statistical approaches to downscaling climate model outputs. Clim. Change 62, 189–216.